Filomat 37:27 (2023), 9431–9446
https://doi.org/10.2298/FIL2327431O

Published by Faculty of Sciences and Mathematics,
University of Niš, Serbia
Available at: http://www.pmf.ni.ac.rs/filomat

Inferential results based on Mellin-type statistics for the transmuted inverse Weibull distribution

Daniel L. R. Orozco[a], Josimar M. Vasconcelos[a], Frank Gomes-Silva[a]

[a]*Programa de Pós Graduação em Biometria e Estatística Aplicada, Departamento de Estatística e Informática, Universidade Federal Rural de Pernambuco, Recife-PE, Brazil*

Abstract. Different measures of goodness-of-fit provide information to describe how well models fit the data. However, it's important to note that these measures have shown modest growth in comparison to the emergence of probability distribution models. That said, this research constructed qualitative and quantitative fit measures for Transmuted Inverse Weibull distribution. To develop these Goodness-of-Fit measures, we study some properties of that distribution: we present the Mellin Transform, Log-Moments, and Log-Cumulants. Then, we discuss estimation methods for the model's parameters, such as Moments, Maximum Likelihood, and the one based on the Log-Cumulants method. The last method mentioned is proposed to estimate the parameters of the distribution. We make the Log-Cumulants diagrams and construct the confidence ellipses. The model is applied to three survival datasets to verify the quality of our estimation methods and Goodness-of-Fit measures.

1. Introduction

Lifetime probability distributions has been used in different contexts, such as reliability [20, 29], life data [27], modeling failure, and engineering [36], among others. Researchers generally introduce parameters or/and generators to obtain more new/flexible models. In this paper, we use a distribution that provides a particular transmuting function for constructing tractable models. The famous Weibull distribution was introduced by Weibull et al. [46] and also mentioned in Rinne [38]. This distribution is mainly used in quality control by Nelson [31] and studied in Hallinan [15], reliability and applied statistics [32, 4], hidrology [41, 39], among others. Nevertheless, in some situations which the fit of simple models to the data are not good, it is necessary to create new models that supply this fact, by adding parameters or baseline distributions, to guarantee the flexibility of the model and better fits. Keller and Arr [21] derived four alternative failure models based on physical considerations, particularly the two-parameter model known as the Inverse Weibull model. Such distribution plays an essential role in modeling failure rates which are extremely important in biological, reliability, and survival analysis studies. Subsequently, some works generalize or modify the inverse Weibull, for example, De Gusmao et al. [11], Khan and King [22], Khan and King [24] and Jan et al. [19].

2020 *Mathematics Subject Classification*. 62Fxx; 63F03,62F10
Keywords. Parameter Estimation, Log-Cumulants, Goodness-of-Fit, Confidence Ellipse
Received: 01 April 2023; Revised: 03 May 2023; Accepted: 30 May 2023
Communicated by Biljana Popović
The research of Daniel Leonardo Ramírez Orozco was supported by the Brazilian Government through the Coordenação de Aperfeiçoamento de Pessoal de Nível Superior (CAPES) Cod. 001.
Email addresses: orozco.dlr@gmail.com (Daniel L. R. Orozco), josimar.vasconcelos@ufrpe.br (Josimar M. Vasconcelos), frank.gsilva@ufrpe.br (Frank Gomes-Silva)

An excellent idea of a generalization model where the distribution is derived using the quadratic rank transmutation map is intended to motivate our investigation; it was given by Shaw and Buckley [40]. In this context, Khan and King [23] introduce the three-parameter Transmuted Inverse Weibull (TIW) distribution, evidencing the Transmuted Inverse Exponential, Transmuted Inverse Rayleigh, and Inverse Weibull distributions as sub-models. Merovci et al.[30] created a new generalized inverse Weibull distribution. Al-Omari [3] developed a new acceptance sampling plan based on the Transmuted Generalized Inverse Weibull distribution. Al-Kadim and Mohammed [2] proposed a cubic Transmuted Weibull distribution, discuss some special cases, and gave theoretical results. Recently, Rahman et al.[37] studied a detailed review of the transmuted families of distributions and Dey et al. [13] reviewed a complete list of transmuted distributions.

Now, let us mention the Mellin Transform (MT); it surges in a mathematical context, the Finnish mathematician R.H.Mellin (1854-1933) was the first to formulate that, and it has been applied in different fields of engineering. Butzer and Jansche [10] show an application to the partial differential equations as a particular use of the differential properties. Nicolas [33] presents an interesting application based on graphic representation using Log-Cumulants (LC) of order two and three, leading to graphing the LC diagram. Recently, Jain et al. [18] introduced a study called a (p, q)-Mellin transform and its corresponding convolution and inversion. They solve some integral equations in terms of applications of the (p, q)-Mellin transform.

Finally, different techniques in the literature help to choose the best fit to the models by using criteria and measures for different distributions, known as Goodness-of-Fit (GoF). So far, no developed GoF measures have been applied to the TIW distribution, making it difficult to select this model in some cases. In this line, Pearson [35] provides an excellent tool for choosing a model known as the Pearson diagram, which uses skewness and kurtosis. However, Nicolas [33] considered this method sometimes analytically intractable. Hence, this author built the LC diagram for some classical models illustrating synthetic aperture radar (SAR) image data. Vasconcelos et al. [45] recently constructed LC diagrams and derived confidence ellipses for the LC for the beta-G class based on Hotelling's T^2 statistic.

In this article, we study the MT to establish new GoF measures for the TIW distribution, with a simple simulation study we compare the Maximum Likelihood, Moments, and LC estimates. Using the T^2 statistic and the confidence ellipses for hypothesis testing, we illustrate the performance of the measures treated in some datasets. This work, aims to give inferential results using new GoF method. To accomplish this, we provide a study specially of the MT, LC and Log-Moments.

The paper is organized as follows: Section 2 presents a brief overview of TIW distribution and the parameters estimation theory. In Section 3 we propose a second kind statistic for the TIW distribution. Section 4 offers Log-Cumulants and T^2 statistics. Section 5 is a short simulation. Section 6 shows an application to a real dataset, and finally, Section 7 presents the conclusions and future work.

2. TIW Distribution

In this section, let us introduce some aspects of the literature of how the TIW could be created.

A random variable Y is said to follow a Weibull distribution [46, 38] with parameters $\beta > 0$ and $\eta > 0$, the scale and shape parameters, respectively, if its cumulative distribution function (CDF) and probability density function (PDF) are,

$$G_Y(y) = 1 - \mathrm{e}^{-\left(\frac{y}{\beta}\right)^{\eta}} \qquad \text{and} \qquad g_Y(y) = \frac{\eta}{\beta}\left(\frac{y}{\beta}\right)^{\eta-1}\mathrm{e}^{-\left(\frac{y}{\beta}\right)^{\eta}}, \quad y \geq 0.$$

Let Z be a random variable following Inverse Weibull distribution, say $Z \sim IW(z; \beta, \eta)$, with parameters $\beta > 0$ and $\eta > 0$, the scale and shape parameters, respectively. The CDF and PDF, respectively, are given by Keller and Arr [21] (see also Khan et al. [25]):

$$G_Z(z) = \mathrm{e}^{-\frac{1}{\eta}\left(\frac{1}{z}\right)^{\beta}}, \qquad \text{and} \qquad g_Z(z) = \left(\frac{\beta}{\eta}\right)\left(\frac{1}{z}\right)^{\beta+1}\mathrm{e}^{-\frac{1}{\eta}\left(\frac{1}{z}\right)^{\beta}}, \quad z > 0.$$

Transmutation is the functional composition of the CDF of one distribution with the inverse cumulative distribution (quantile function) of another [37]. A random variable W is said to follow transmuted distribution, see Shaw and Buckley [40], if its CDF is given by

$$F_W(w) = (1+\lambda)G(w) - \lambda G(w)^2, \qquad |\lambda| \leq 1, \tag{1}$$

where λ offers more flexibility in the distribution and $G(w)$ is the CDF of the baseline distribution.

Finally, this distribution arises like a new reliability model. From (1), a random variable X is said to follow the TIW distribution denoted by, $X \sim TIW(x;\beta,\eta,\lambda)$ if the CDF and PDF of X are given by

$$F_X(x) = (1+\lambda)\,\mathrm{e}^{-\frac{1}{\eta}\left(\frac{1}{x}\right)^{\beta}} - \lambda\left(\mathrm{e}^{-\frac{1}{\eta}\left(\frac{1}{x}\right)^{\beta}}\right)^2,$$

$$f_X(x) = \left(\frac{\beta}{\eta}\right)\left(\frac{1}{x}\right)^{\beta+1}\mathrm{e}^{-\frac{1}{\eta}\left(\frac{1}{x}\right)^{\beta}}\left(1+\lambda-2\lambda\,\mathrm{e}^{-\frac{1}{\eta}\left(\frac{1}{x}\right)^{\beta}}\right), \qquad x>0.$$

Where $\beta, \eta > 0$, and $|\lambda| \leq 1$, the shape, scale and transmuting parameters, respectively [23].

Figure 1 illustrates the flexibility of the CDF and PDF for selected parameter values. Note that, when $\lambda = 0.04$ the density is a monotonic function and when $\beta > 1.5$ becomes unimodal. When x tends to infinity the density tends to zero. Now, when λ is close to 1 has a leptokurtic form already in the case of $\lambda < 1$ as it decreases has a platykurtic shape.

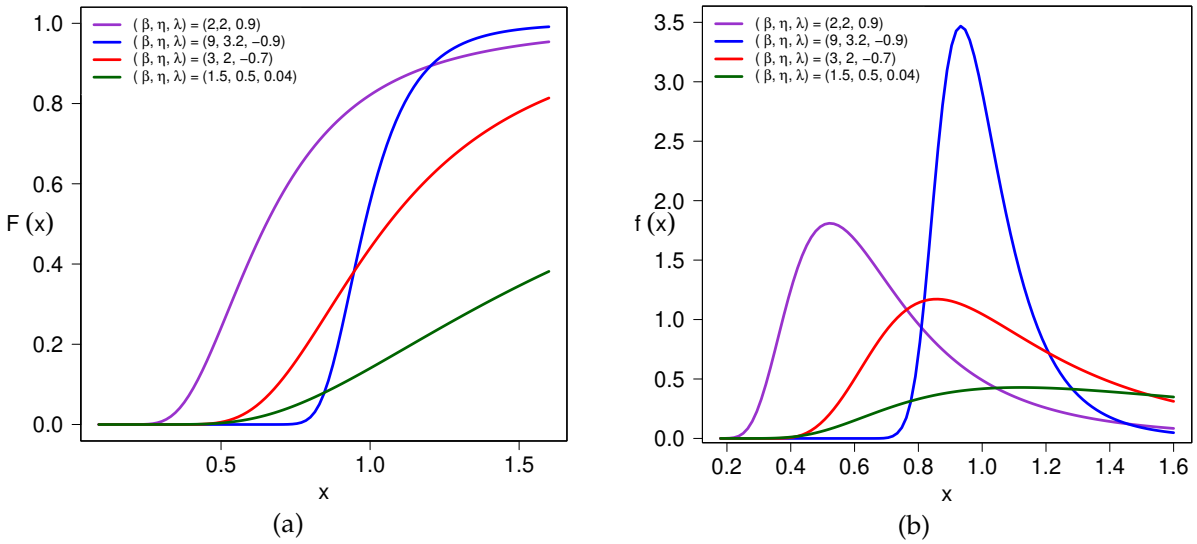

Figure 1: TIW CDF (a) and PDF (b) for different values of β, η, λ

To generate data from a probability distribution we need some methodology. One of them is by quantile function when it is possible to find the inverse of the CDF. Then, using u a random number from zero to one, the quantile function from TIW, by solving $F_X(x) \leq u$ is

$$x = \left[-\eta\log\left(\frac{(1+\lambda) - \sqrt{(1+\lambda)^2 - 4\lambda u}}{2\lambda}\right)\right]^{\frac{-1}{\beta}}.$$

If $u = 0.5$, we obtain the median of the TIW distribution. In practice, this is the life at which at least 50% of the units will be expected to fail.

To estimate the parameters of TIW distribution, we present in this section two methods: the Maximum Likelihood and Moments.

2.1. Method of Maximum Likelihood

Let $X_1, X_2, \ldots, X_n$ be a random sample from $X \sim TIW(x; \beta, \eta, \lambda)$. The likelihood function is

$$L(\beta, \eta, \lambda; x_i) = \prod_{i=1}^{n} \frac{\beta}{\eta} \left(\frac{1}{x_i}\right)^{\beta+1} \mathrm{e}^{-\frac{1}{\eta}\left(\frac{1}{x_i}\right)^{\beta}} \left(1 + \lambda - 2\lambda\, \mathrm{e}^{-\frac{1}{\eta}\left(\frac{1}{x_i}\right)^{\beta}}\right), \tag{2}$$

where $x_i, i = 1, 2, \ldots, n$ are the observed values of the random sample.

To estimate the parameters, we find the set of values of β, η and λ that attains their maximum in (2).

The associated log-likelihood function of (2) is

$$\ell(\beta, \eta, \lambda; x_i) = n \log \frac{\beta}{\eta} + (\beta + 1) \sum_{i=1}^{n} \log\left(\frac{1}{x_i}\right) - \sum_{i=1}^{n} \frac{1}{\eta}\left(\frac{1}{x_i}\right)^{\beta} + \sum_{i=1}^{n} \log\left(1 + \lambda - 2\lambda\, \mathrm{e}^{-\frac{1}{\eta}\left(\frac{1}{x_i}\right)^{\beta}}\right). \tag{3}$$

The values of $\hat{\beta}, \hat{\eta}$ and $\hat{\lambda}$ that maximize (3) will be the Maximum Likelihood (ML) estimates for the parameters β, η and λ. The ML estimates can be obtained by numerical methods using the `optim` function, `BFGS` method and `BB` package [44] in the software R Core Team [43]. The corresponding components of the score vector $\mathbb{S}$, by taking the partial derivates of (3) can be written as

$$\mathbb{S} = \left(\mathbb{S}_\beta, \mathbb{S}_\eta, \mathbb{S}_\lambda\right) = \left(\frac{\partial}{\partial\beta}\ell(\beta, \eta, \lambda; x_i), \frac{\partial}{\partial\eta}\ell(\beta, \eta, \lambda; x_i), \frac{\partial}{\partial\lambda}\ell(\beta, \eta, \lambda; x_i)\right),$$

where

$$\begin{aligned}
\frac{\partial}{\partial\beta}\ell(\beta, \eta, \lambda; x_i) &= \frac{n}{\beta} + 2\sum_{i=1}^{n} \frac{\lambda\left(\frac{1}{x_i}\right)^{\beta} \log\left(\frac{1}{x_i}\right) \mathrm{e}^{-\left(\frac{1}{\eta}\right)\left(\frac{1}{x_i}\right)^{\beta}}}{\eta\left(\lambda - 2\lambda\, \mathrm{e}^{-\frac{1}{\eta}\left(\frac{1}{x_i}\right)^{\beta}} + 1\right)} - \frac{1}{\eta}\sum_{i=1}^{n}\left(\frac{1}{x_i}\right)^{\beta} \log\left(\frac{1}{x_i}\right) + \sum_{i=1}^{n} \log\left(\frac{1}{x_i}\right), \\
\frac{\partial}{\partial\eta}\ell(\beta, \eta, \lambda; x_i) &= -\frac{n}{\eta} - 2\sum_{i=1}^{n} \frac{\lambda\left(\frac{1}{x_i}\right)^{\beta} \mathrm{e}^{-\left(\frac{1}{\eta}\right)\left(\frac{1}{x_i}\right)^{\beta}}}{\eta^2\left(\lambda - 2\lambda\, \mathrm{e}^{-\frac{1}{\eta}\left(\frac{1}{x_i}\right)^{\beta}} + 1\right)} + \frac{1}{\eta^2}\sum_{i=1}^{n}\left(\frac{1}{x_i}\right)^{\beta}, \\
\frac{\partial}{\partial\lambda}\ell(\beta, \eta, \lambda; x_i) &= \sum_{i=1}^{n} \frac{1 - 2\,\mathrm{e}^{-\left(\frac{1}{\eta}\right)\left(\frac{1}{x_i}\right)^{\beta}}}{\lambda - 2\lambda\, \mathrm{e}^{-\left(\frac{1}{\eta}\right)\left(\frac{1}{x_i}\right)^{\beta}} + 1}.
\end{aligned}$$

Remark 2.1. *We consider that there is an error when writing the partial derivative of λ in Khan and King [23] page 281, equation (36).*

2.2. Method of Moments

The method of moments (MM), is an estimation method of population parameters. It involves equaling sample moments with theoretical moments. For $r > 0$ integer, the r-th sample moment is the random variable

$$\mathbb{E}(X^r) = \frac{1}{n}\sum_{i=1}^{n} X_i^r = \mu_r.$$

Let $X_1, X_2, \ldots, X_n$ be a random sample from $X \sim TIW(x; \beta, \eta, \lambda)$. The r-th moment is given as follows

$$\mathbb{E}\left(X^r\right) = \eta^{\,\frac{r}{\beta}}\Gamma\left(1 - \frac{r}{\beta}\right)\left(1 + \lambda - \lambda 2^{\frac{r}{\beta}}\right), \tag{4}$$

where $\Gamma(\cdot)$ is the Gamma function.

Thus, for $r = 1, 2, 3$ in (4) and solving by numerical methods these equations, we can obtain the MM estimates. The `dfsane` function, `BFGS` method and `BB` package were used in the software R Core Team [43].

3. Second Kind Statistics for the TIW Distribution

In this section, we present one of our results for TIW distribution based on the Mellin Transform. The next, we will review some results from literature and then present the new results for TIW distribution.

3.1. Mellin Transform

The MT relates to Laplace and Fourier transforms, and has been applied in different engineering fields [9]. Let X be a positive random variable and CDF $F(x)$. The first characteristic function of the second kind is defined from the MT, denoted by $\phi_X(s)$ [14, 33]

$$\phi_X(s) = \int_0^\infty x^{s-1} dF(x) = \mathbb{E}\left(X^{s-1}\right). \tag{5}$$

Generally, the above integral does exist only for $s = a + bj$, with $a, b \in \mathbb{R}$ and j the imaginary number.

The second characteristic function of the second kind, denoted by $\varphi_X(s)$, is defined as the natural logarithm of (5)

$$\varphi_X(s) = \log\left(\phi_X(s)\right). \tag{6}$$

With this we motivation to formulate the next results.

Theorem 3.1. *Let X be a random variable following TIW distribution, $X \sim TIW(x; \beta, \eta, \lambda)$. The MT of X is given by*

$$\phi_X(s) = \eta^{-\frac{s-1}{\beta}} \Gamma\left(1 - \frac{s-1}{\beta}\right)\left(1 + \lambda - \lambda 2^{\frac{s-1}{\beta}}\right). \tag{7}$$

The proof of Theorem 3.1 follows immediately from (4) and (5).

3.2. Log-Cumulants

There is a closely related between Log-Moments (LM) and LC. Now, we show LM are derived from MT similarly that the moments are obtained from the characteristic function.

Nicolas [33] defines $\forall r \in \mathbb{N}$, the r-th LM or second-kind moment of the MT as following

$$\tilde{\mu}_r = \frac{d^r \phi_X}{ds^r}(s)\bigg|_{s=1} = \int_0^\infty (\log x)^r dF(x) = \mathbb{E}\left((\log X)^r\right).$$

The r-th LC is obtained from derivative of (6) and then by evaluating the function at $s = 1$,

$$\tilde{\kappa}_r = \frac{d^r \varphi_X(s)}{ds^r}\bigg|_{s=1}. \tag{8}$$

Thus, the expressions for the r-th LC [7] are given by

$$\begin{aligned}
\tilde{\kappa}_1 &= \tilde{\mu}_1, \\
\tilde{\kappa}_2 &= \tilde{\mu}_2 - \tilde{\mu}_1^2, \\
\tilde{\kappa}_3 &= \tilde{\mu}_3 - 3\tilde{\mu}_1\tilde{\mu}_2 + 2\tilde{\mu}_1^3, \\
&\vdots \\
\tilde{\kappa}_r &= \tilde{\mu}_r - \sum_{i=1}^{r-1} \binom{r-1}{i-1} \tilde{\kappa}_i \tilde{\mu}_{r-i},
\end{aligned} \tag{9}$$

where $\tilde{\mu}_r$ can be replaced by [34]

$$\hat{\tilde{\mu}}_r = \frac{1}{n}\sum_{i=1}^{n}(\log x_i)^r, \tag{10}$$

where, n is the sample size and x_i indicates the i-th sample observation.

In Table 1, for $X \sim TIW(x;\beta,\eta,\lambda)$ we present the first six theoretical LCs, where the polygamma function of order n, $\Psi^{(n)}(x) = \frac{d^{n+1}}{dx^{n+1}}\log\Gamma(x)$, is the $(n+1)$-th derivative of the logarithm of the gamma function. Thus, the $\varphi_X(s)$ function for TIW distribution can be written as

$$\varphi_X(s) = (1-s)\frac{1}{\beta}\log(\eta) + \log\left(\Gamma\left(1-\frac{s-1}{\beta}\right)\right) + \log\left(1+\lambda-\lambda 2^{\frac{s-1}{\beta}}\right). \tag{11}$$

LC	$-\mathbf{1} < \lambda < \mathbf{1}$
$\tilde{\kappa}_1$	$-\frac{1}{\beta}\left[\log(\eta) + \lambda\log(2) + \Psi^{(0)}(1)\right]$
$\tilde{\kappa}_2$	$-\frac{1}{\beta^2}\left[\lambda\log^2(2)(\lambda+1) - \Psi^{(1)}(1)\right]$
$\tilde{\kappa}_3$	$-\frac{1}{\beta^3}\left[\lambda\log^3(2)\left(2\lambda^2+3\lambda+1\right) + \Psi^{(2)}(1)\right]$
$\tilde{\kappa}_4$	$-\frac{1}{\beta^4}\left[\lambda\log^4(2)\left(6\lambda^3+12\lambda^2+7\lambda+1\right) - \Psi^{(3)}(1)\right]$
$\tilde{\kappa}_5$	$-\frac{1}{\beta^5}\left[\lambda\log^5(2)\left(24\lambda^4+60\lambda^3+50\lambda^2+15\lambda+1\right) + \Psi^{(4)}(1)\right]$
$\tilde{\kappa}_6$	$-\frac{1}{\beta^6}\left[\lambda\log^6(2)\left(120\lambda^5+360\lambda^4+390\lambda^3+180\lambda^2+31\lambda+1\right) - \Psi^{(5)}(1)\right]$

Table 1: The first six LCs of the TIW distribution

4. Estimation and GoF for the TIW Distribution

4.1. Method of Log-Cumulants

In a similar way to Subsection 2.2, the proposed estimation method consists in equaling sample version LCs in (10) with theoretical LCs according to (9) as follow

$$\begin{aligned}
-\frac{1}{\hat{\beta}}\left[\log(\hat{\eta}) + \hat{\lambda}\log(2) + \Psi^{(0)}(1)\right] &= \hat{\tilde{\mu}}_1,\\
-\frac{1}{\hat{\beta}^2}\left[\hat{\lambda}\log^2(2)(\hat{\lambda}+1) - \Psi^{(1)}(1)\right] &= \hat{\tilde{\mu}}_2 - \hat{\tilde{\mu}}_1^2,\\
-\frac{1}{\hat{\beta}^3}\left[\hat{\lambda}\log^3(2)\left(2\hat{\lambda}^2+3\hat{\lambda}+1\right) + \Psi^{(2)}(1)\right] &= \hat{\tilde{\mu}}_3 - 3\hat{\tilde{\mu}}_1\hat{\tilde{\mu}}_2 + 2\hat{\tilde{\mu}}_1^3.
\end{aligned}$$

By using above equalities and after some algebraic manipulations, we get

$$\begin{aligned}
\hat{\beta} &= \sqrt[3]{\frac{\hat{\lambda}\left(2\hat{\lambda}^2+3\hat{\lambda}+1\right)\log^3(2) + \Psi^{(2)}(1)}{-\hat{\tilde{\mu}}_3 + 3\hat{\tilde{\mu}}_1\hat{\tilde{\mu}}_2 - 2\hat{\tilde{\mu}}_1^3}},\\
\hat{\eta} &= \mathrm{e}^{-\hat{\beta}\hat{\tilde{\mu}}_1 - \hat{\lambda}\log(2) - \Psi^{(0)}(1)},\\
\hat{\lambda} &= \frac{2\cdot\sqrt{-\hat{\beta}^2\left(\hat{\tilde{\mu}}_2 - \hat{\tilde{\mu}}_1^2\right) - \Psi^{(1)}(1)} - \log(2)}{2\log(2)}.
\end{aligned}$$

Remark 4.1. *An advantage of this method is that there is an expression in closed form. This does not happen in the above methods. Thus, the system is solved by non-linear optimization methods.*

This study was carried out by using the `BB` and `MaxLik` packages Varadhan and Gilbert [44] and Henningsen and Toomet [16], also by using `BBsolve`, `maxBFGS` functions avaliables in the software R Core Team.

4.2. The Log-Cumulant Diagram

Let us start this section by mentioning that the Pearson system [12] helps in the model selection and choosing the best fit for the data based on kurtosis and skewness measures. Nevertheless, Nicolas [33] showed that the Pearson diagram sometimes could be complex in treating positive random variables and introduced the $(\tilde{\kappa}_3, \tilde{\kappa}_2)$ diagram, which uses the second statistics $\tilde{\kappa}_3$ and $\tilde{\kappa}_2$ rather than kurtosis and skewness measures.

There are different representations in the diagram due to the number of parameters contained in LC expressions [7]. Hence, when there is no parameter in LC expressions, there is a zero-dimensional space; one parameter in LC is represented by a curve and a surface for two parameters.

Figure 2 displays the 2-dimensional space representing the third-order LC versus the second-order LC, referring to the TIW distribution. Here, we can plot the region obtained from the theoretical LC estimated. In application Section 6, the points representing the sample LC will be computed using a bootstrap method from data samples and graphed over the (κ_3, κ_2) diagram.

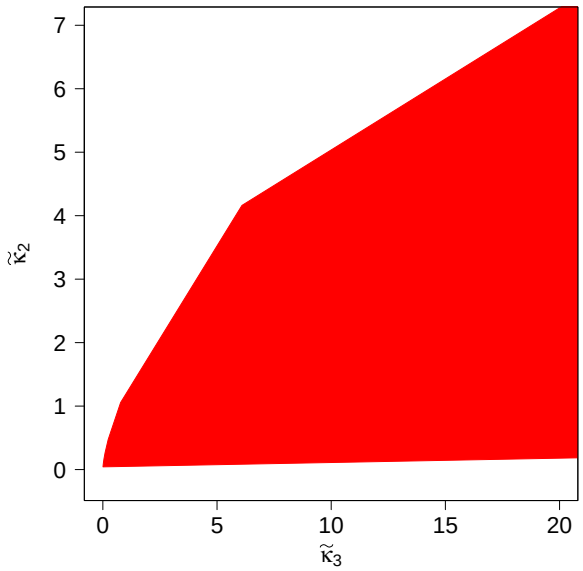

Figure 2: LC Diagram showing the dimensional space of theoretical LC for the TIW distribution

4.3. Hotelling's Statistic

By the multivariate central limit theorem we know that for larger samples sizes, $\sqrt{\mathbf{n}}\left(\bar{\mathbf{X}} - \mu\right) \overset{\text{approx}}{\sim} \mathbb{N}(\mathbf{0}, \mathbf{\Sigma})$, and the covariance matrix follows a chi-square distribution with ν degrees of freedom, denoted by

$$\mathbf{\Sigma} = n\left(\bar{\mathbf{X}} - \mu\right)^{\top} \mathbf{S^{-1}} \left(\bar{\mathbf{X}} - \mu\right) \overset{\text{approx}}{\sim} \chi^{2}_{\nu},$$

where μ is the mean vector, $\bar{\mathbf{X}}$ is the sample mean vector and $\mathbf{S}$ is the sample covariance matrix. Now, the t-student distribution is used for small samples sizes. We can write $t = \frac{\bar{X}-\mu}{s/\sqrt{n}}$, as $T = \sqrt{n}\left(\bar{\mathbf{X}} - \mu\right)\mathbf{S^{-1}}$. If we take square to both terms, we obtain

$$T^2 = n\left(\bar{\mathbf{X}} - \mu\right)^{\top} \mathbf{S^{-1}} \left(\bar{\mathbf{X}} - \mu\right). \tag{12}$$

In this case, (12) will be Hotelling's T^2 statistic [5, 17]. T^2 follows the F-Snedecor distribution with $\nu, n - \nu$ degrees of freedom denoted by $T^2 \sim F_{\nu, n-\nu}$.

Let us consider the next hypothesis testing:

$$H_0 := \mathbb{E}\left(\bar{\mathbf{X}}\right) = \mu \quad \text{vs} \quad H_1 := \mathbb{E}\left(\bar{\mathbf{X}}\right) \neq \mu. \tag{13}$$

Assume the null hypothesis H_0 true and a significance level α. The likelihood ratio test does not reject H_0, will be $T^2 \leq Q(1-\alpha; \nu, n-\nu)$, where $Q(\bullet; \nu, n-\nu)$ is the quantile function for $F_{\nu;n-\nu}$ [5].

We aim to find the Hotelling's T^2 statistic to provide GoF tests using LC. Thus, we pretend to estimate the LC to identify the underlying distribution according to the location of the LC estimated $\left[\hat{\tilde{\kappa}}_2 \quad \hat{\tilde{\kappa}}_3\right]$ over the LC diagram [45].

An equivalent formulation of (13) will be needed

$$H_0 := \mathbb{E}\left(\left[\hat{\tilde{\kappa}}_2 \quad \hat{\tilde{\kappa}}_3\right]\right) = \left[\tilde{\kappa}_2 \quad \tilde{\kappa}_3\right] \quad \text{vs} \quad H_1 := \mathbb{E}\left(\left[\hat{\tilde{\kappa}}_2 \quad \hat{\tilde{\kappa}}_3\right]\right) \neq \left[\tilde{\kappa}_2 \quad \tilde{\kappa}_3\right].$$

To reject or not the null hypothesis depends on the belonging of the LC estimated over the specific regions into the LC diagram [6]. Thus, T^2 converges in distribution to a random variable following a chi-squared distribution with ν degrees of freedom

$$T^2 = n\left(\begin{bmatrix}\hat{\tilde{\kappa}}_2\\ \hat{\tilde{\kappa}}_3\end{bmatrix} - \begin{bmatrix}\tilde{\kappa}_2\\ \tilde{\kappa}_3\end{bmatrix}\right)^{\top} \widehat{\mathbf{K}}^{-1} \left(\begin{bmatrix}\hat{\tilde{\kappa}}_2\\ \hat{\tilde{\kappa}}_3\end{bmatrix} - \begin{bmatrix}\tilde{\kappa}_2\\ \tilde{\kappa}_3\end{bmatrix}\right) \xrightarrow{D} \chi^2_{2,\nu},$$

where $\widehat{\mathbf{K}}$ is the asymptotic covariance matrix and $\mathbb{P}\left(T^2 \leq \chi^2_{2,\nu}\right) = 1-\nu$.

For the ellipse confidences, if μ is the mean of the normal multivariate distribution, that is, $\mathbb{N}(\mu, \mathbf{\Sigma})$, the probability is $1-\alpha$ of drawing a sample of the population with mean $\bar{X}$ and covariance matrix $\mathbf{S}$ such that

$$n\left(\bar{\mathbf{X}} - \mu\right)^{\top} \mathbf{S^{-1}} \left(\bar{\mathbf{X}} - \mu\right) \leq \mathbf{T^2}(\alpha). \tag{14}$$

Thus, if we compute (14) for a particular sample, we have confidence $1-\alpha$ that (14) is a true statement concerning μ [5].

The inequality

$$n\left(\begin{bmatrix}\hat{\tilde{\kappa}}_2\\ \hat{\tilde{\kappa}}_3\end{bmatrix} - \begin{bmatrix}\tilde{\kappa}_2\\ \tilde{\kappa}_3\end{bmatrix}\right)^{\top} \widehat{\mathbf{K}}^{-1} \left(\begin{bmatrix}\hat{\tilde{\kappa}}_2\\ \hat{\tilde{\kappa}}_3\end{bmatrix} - \begin{bmatrix}\tilde{\kappa}_2\\ \tilde{\kappa}_3\end{bmatrix}\right) \leq T^2(\alpha),$$

is the interior and boundary of an ellipsoid of $[\tilde{\kappa}_2, \tilde{\kappa}_3]^{\top}$, with center at $\left[\hat{\tilde{\kappa}}_2, \hat{\tilde{\kappa}}_3\right]^{\top}$ and with size and shape depending on $\widehat{\mathbf{K}}^{-1}$ and α.

Proposition 4.2. *Let X be a random variable following TIW distribution, $X \sim TIW(x; \beta, \eta, \lambda)$. The T^2 statistic based on LC Estimated is given by*

$$T^2 = \frac{n\beta^6}{\hat{\tau}_{33}\hat{\tau}_{22} - \hat{\tau}^2_{23}} \left[\hat{\tau}_{33}\left(\hat{\tilde{\kappa}}_2 - \tilde{\kappa}_2\right)^2 + \hat{\tau}_{22}\left(\hat{\tilde{\kappa}}_3 - \tilde{\kappa}_3\right)^2 - 2\hat{\tau}_{23}\left(\hat{\tilde{\kappa}}_2 - \tilde{\kappa}_2\right)\left(\hat{\tilde{\kappa}}_3 - \tilde{\kappa}_3\right)\right].$$

The proof of Proposition 4.2 and the algorithm to calculate T^2 is in Appendix, Section 8.

5. Simulation Study

We present a brief simulation study to verify the performance of the estimators. We use the ML, MM and LC methods for parameter estimation. Some scenarios with different sample sizes are shown in Table 2.

A simple simulation study with 1000 Monte Carlo experiments is discussed to evaluate the performance of the MM, ML, and LC estimates with different sample sizes such as 30, 50, 80 and 100. In all scenarios, we can observe good results associated with small values; small bias and mean squared error (MSE) values are associated with 80 and 100 sample sizes. We can observe that while the sample size increases, the bias and MSE decrease. However, for the last scenario, MM allows us to see that for λ values close to zero in the third parameter, the MSE is higher. This indicates that it is not a good estimate.

n	(β, η, λ)		MM			ML			LC		
			$\widehat{\beta}$	$\widehat{\eta}$	$\widehat{\lambda}$	$\widehat{\beta}$	$\widehat{\eta}$	$\widehat{\lambda}$	$\widehat{\beta}$	$\widehat{\eta}$	$\widehat{\lambda}$
30	(2, 2, 0.9)	Mean	2.903	4.306	0.818	2.509	3.803	0.772	2.414	3.554	0.882
		Bias	0.903	2.306	-0.082	0.509	1.803	-0.128	0.414	1.554	-0.018
		MSE	1.662	48.876	0.268	0.975	40.529	0.132	1.111	14.901	0.131
50			2.590	2.880	0.895	2.236	2.747	0.755	2.163	2.997	0.810
			0.590	0.880	-0.005	0.236	0.747	-0.145	0.163	0.997	-0.090
			0.807	4.865	0.194	0.277	3.118	0.138	0.468	9.312	0.165
80			2.498	2.576	0.926	2.179	2.582	0.767	2.104	2.731	0.812
			0.498	0.576	0.026	0.179	0.582	-0.133	0.104	0.731	-0.088
			0.625	2.996	0.183	0.188	2.062	0.129	0.334	6.250	0.166
100			2.409	2.348	0.965	2.139	2.490	0.768	2.097	2.707	0.779
			0.409	0.348	0.065	0.139	0.490	-0.132	0.097	0.707	-0.121
			0.516	2.049	0.171	0.129	1.535	0.127	0.280	5.275	0.180
30	(9, 3.2, −0.9)		10.662	2.304	-0.281	9.303	1.952	-0.046	9.492	1.960	-0.057
			1.662	-0.896	0.619	0.303	-1.248	0.854	0.492	-1.240	0.843
			12.729	2.206	1.029	8.271	2.230	1.379	10.572	2.426	1.313
50			9.908	2.668	-0.551	9.079	2.542	-0.481	9.286	2.538	-0.473
			0.908	-0.532	0.349	0.079	-0.658	0.419	0.286	-0.662	0.427
			4.538	1.260	0.506	2.256	1.026	0.568	3.738	1.126	0.541
80			9.703	2.836	-0.653	9.095	2.723	-0.601	9.246	2.746	-0.602
			0.703	-0.364	0.247	0.095	-0.477	0.299	0.246	-0.454	0.298
			3.143	1.067	0.365	1.360	0.703	0.347	2.518	0.826	0.337
100			9.485	2.981	-0.742	9.110	2.895	-0.713	9.174	2.960	-0.732
			0.485	-0.219	0.158	0.110	-0.305	0.187	0.174	-0.240	0.168
			1.897	0.898	0.250	0.663	0.437	0.170	1.398	0.593	0.178
30	(3, 2, −0.7)		4.334	2.209	-0.175	3.447	1.988	-0.573	3.812	2.088	-0.619
			1.334	0.209	0.525	0.447	-0.012	0.127	0.812	0.088	0.081
			4.624	15.403	4.930	1.226	0.739	0.199	2.186	1.277	0.113
50			3.722	2.159	-0.050	3.080	2.106	-0.720	3.264	2.134	-0.717
			0.722	0.159	0.650	0.080	0.106	-0.020	0.264	0.134	-0.017
			1.935	3.172	7.380	0.231	0.294	0.096	0.559	0.627	0.120
80			3.592	2.118	-0.129	3.016	2.133	-0.756	3.157	2.133	-0.736
			0.592	0.118	0.571	0.016	0.133	-0.056	0.157	0.133	-0.036
			1.442	2.989	3.730	0.119	0.222	0.072	0.324	0.494	0.113
100			3.497	2.085	-0.252	2.980	2.145	-0.769	3.083	2.134	-0.743
			0.497	0.085	0.448	-0.020	0.145	-0.069	0.083	0.134	-0.043
			1.073	2.180	2.396	0.060	0.173	0.059	0.175	0.392	0.103
30	(1.5, 0.5, 0.04)		1.499	1.310	0.613	1.655	0.462	0.212	2.102	0.519	0.383
			-0.001	0.810	0.573	0.155	-0.038	0.172	0.602	0.019	0.343
			0.001	1.504	41.762	0.301	0.032	0.251	0.947	0.064	0.278
50			1.494	0.939	0.730	1.465	0.473	0.253	1.730	0.552	0.282
			-0.006	0.439	0.690	-0.035	-0.027	0.213	0.230	0.052	0.242
			0.000	0.546	55.592	0.082	0.017	0.264	0.268	0.026	0.269
80			1.494	0.795	0.670	1.425	0.473	0.269	1.641	0.565	0.247
			-0.006	0.295	0.630	-0.075	-0.027	0.229	0.141	0.065	0.207
			0.000	0.246	19.319	0.058	0.013	0.259	0.162	0.021	0.262
100			1.495	0.682	0.812	1.407	0.474	0.274	1.568	0.569	0.184
			-0.005	0.182	0.772	-0.093	-0.026	0.234	0.068	0.069	0.144
			0.000	0.087	31.224	0.046	0.010	0.250	0.095	0.017	0.253

Table 2: Parameter estimates for TIW distribution in some scenarios

6. Application to Real Datasets

In this section, we provide an analysis of real datasets to evaluate the T^2 statistic. In the present study, we will be using the following three datasets:

- DATASET 1: The data are taken from Aarset [1] and also reported in Khan and King [23], which refers to the failure times of fifty devices put on life tests at time zero. This dataset is known to have a bathtub-shaped hazard rate.
- DATASET 2: The data in Lee and Wang [28] represents a set of reported remission times (in months) of 128 bladder cancer patients.
- DATASET 3: The data are the time between failures (thousands of hours) of 23 secondary reactor pumps installed in the RSG-GAS reactor [42, 8].

For the above datasets, in Table 3 we show some descriptive statistics for each one. Coefficient of Variation (CV) values indicate greater levels of dispersion in data around the mean. Related to asymmetry and kurtosis in dataset 1, they indicate left tail and smooth distribution, respectively. In dataset 2, for the mean, median, and mode values, we have left skewed distribution. Standard Deviation (SD) in dataset 3 observations indicate a low dispersed relation to the mean.

Values in Table 4 illustrate the T^2 statistic and p-value in each dataset. We verify the quality of our estimation methods and GoF measures in all estimation methods.

Dataset	Min	Max	Mean	Median	Moda	SD	Asymmetry	Kurtosis	CV
1	0.10	86.00	45.69	48.50	1.00	32.84	-0.13	-1.64	71.87
2	0.08	79.05	9.37	6.39	5.32	10.51	3.29	18.48	112.20
3	0.06	6.56	1.55	0.61	0.75	1.97	1.29	0.18	127.10

Table 3: Descriptive statistics for datasets

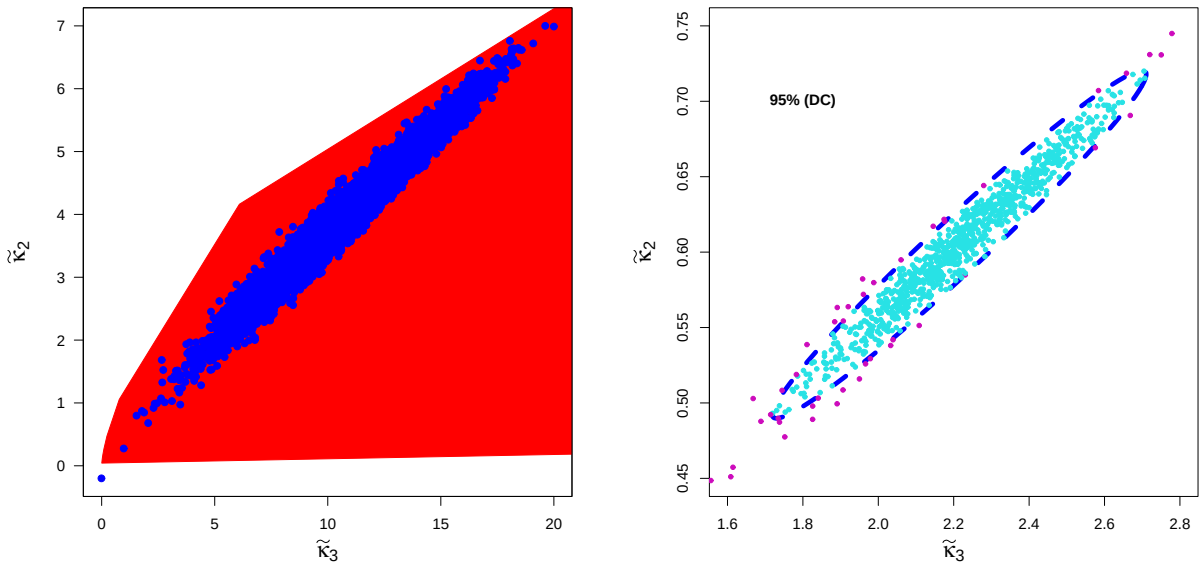

(a) (b)

Figure 3: Diagram of the LC $(\tilde{\kappa}_3, \tilde{\kappa}_2)$ and Confidence Ellipses for the dataset 1 for TIW distribution

As an additional analysis, we show a visual illustration form of fits with confidence ellipses for each dataset. To plot the points in each figure, they were obtained by the bootstrap method with 1000 replicates. We use the T^2 statistic value to measure the distance between the data and the TIW model. The better fit between the data and the model means a smaller T^2 statistic and consequently a higher p-value indicates do not reject the null hypothesis. The ellipse center will be the LCs $\left[\hat{\tilde{\kappa}}_2, \hat{\tilde{\kappa}}_3\right]^\top$ and the axes are directed according to the eigenvectors of $\widehat{\mathbf{K}}$; the Degree Coverage (DC) is quantified with a significance level of 95%. See Figures 3, 4 and 5.

For Dataset 1, the MM and LC methods have a p-value greater than the ML method, and also T^2 is remarkably higher than the last method. Figure 3 shows the majority of points into the diagram and into the ellipse. As a similar way, Figure 4 shows most of the points over the diagram and the ellipse. That means a good fit. T^2 for Dataset 2 has a smaller value in the LC method than others, and seeing the p-value higher means the best fit, such that Dataset 3 have the similar analysis. However, in Figure 5, despite the points perpendicular to the diagram, they are over the diagram and most of them are over the ellipse.

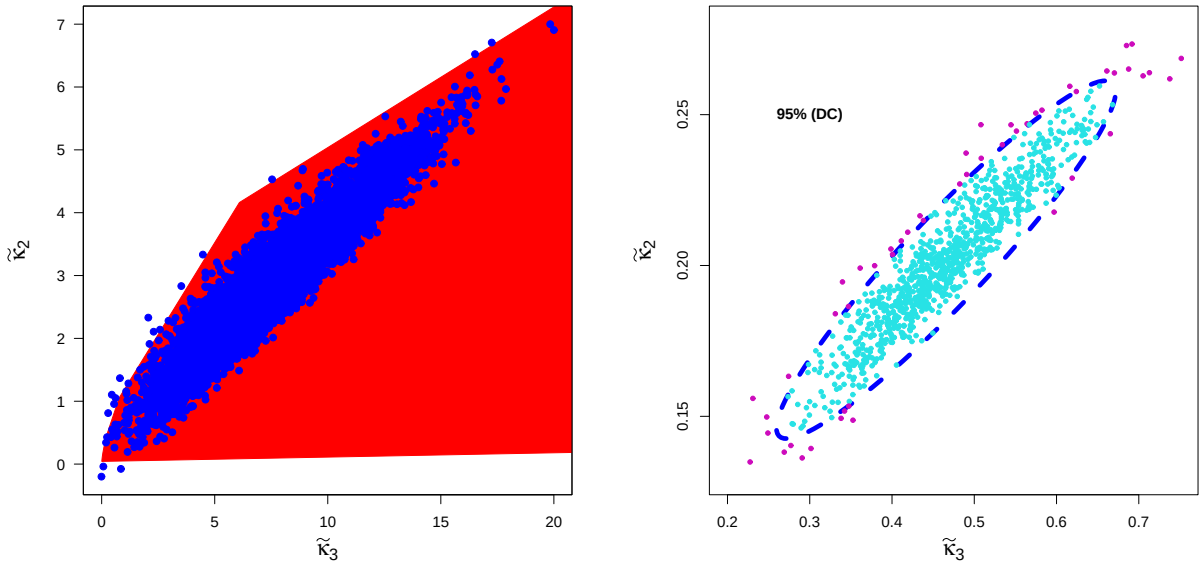

(a) (b)

Figure 4: Diagram of the LC $(\tilde{\kappa}_3, \tilde{\kappa}_2)$ and Confidence Ellipses for the dataset 2 for TIW distribution

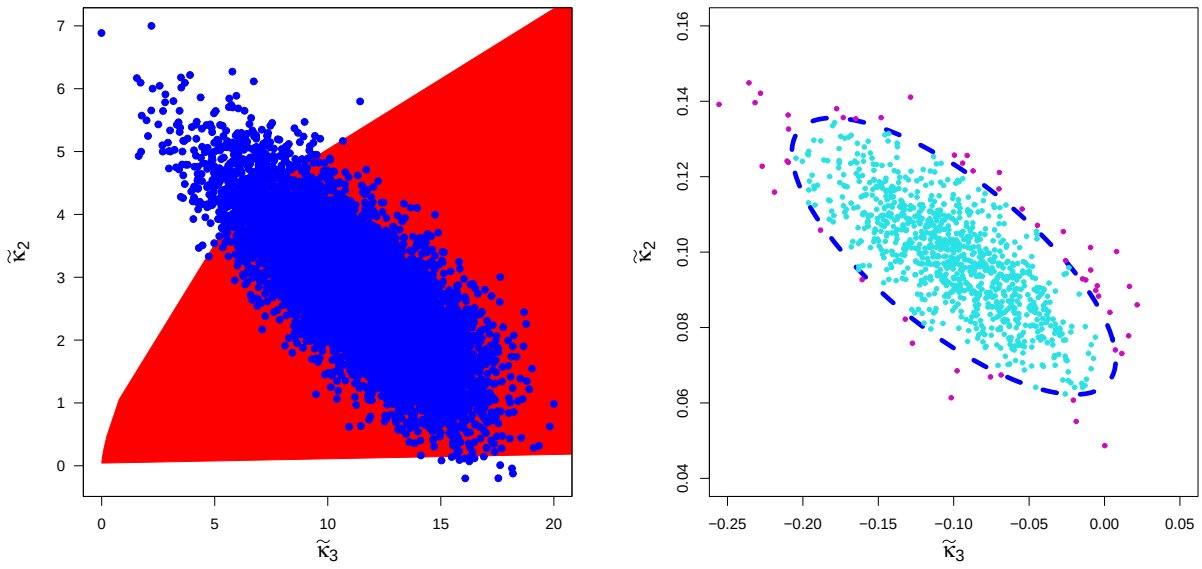

(a) (b)

Figure 5: Diagram of the LC $(\tilde{\kappa}_3, \tilde{\kappa}_2)$ and Confidence Ellipses for the dataset 3 for TIW distribution

7. Some conclusions and future work

We provide analitical and visual analysis to Goodness-of-Fit measures to the datasets. We furnish the Mellin Transform for Transmuted Inverse Weibull distribution and present the closed form expressions for Log-Cumulants estimators. We estimate the parameters model using Maximum Likelihood, Moments and

Method	Dataset 1			Dataset 2			Dataset 3		
	Estimative $(\hat{\beta}, \hat{\eta}, \hat{\lambda})$	T^2	p-value	Estimative $(\hat{\beta}, \hat{\eta}, \hat{\lambda})$	T^2	p-value	Estimative $(\hat{\beta}, \hat{\eta}, \hat{\lambda})$	T^2	p-value
MM	0.750 2.194 -0.422	1.521	0.693	0.749 2.155 -0.477	8.196	0.049	1.487 1.647 -0.101	0.348	0.956
ML	0.512 0.518 -0.700	10.220	0.029	0.835 0.639 -0.855	4.092	0.263	0.847 3.262 -0.442	1.675	0.683
LC	2.468 0.001 -0.796	0.276	0.966	2.447 0.034 -0.533	0.181	0.980	1.429 4.698 -0.578	0.298	0.964

Table 4: Estimatives, T^2 statistic and p-value for the datasets.

Log-Cumulants and show the better fit in the specific dataset by T^2 statistic and ellipses confidence. A simple Monte Carlo simulation study accomplished the performance estimators.

For future work, we recommend doing a comparative study analyzing the parameters of other families of distributions such as the corrected Kies distribution because of its flexibility (see [47]). Also, in order to choose an appropriate model that best fits to the data, it is important to know intrinsic characteristics such as saturation in the sense of Hausdorff see [26]. Estimates of the value of the best Hausdorff approximation of the shifted Heaviside function and the cumulative distribution function of Transmuted Inverse Weibull could be used in practice as a possible additional criterion.

8. Appendix

8.1. Quantile function of TIW

$$
\begin{aligned}
F_X(x) &= u \\
(1+\lambda)\,\mathrm{e}^{-\frac{x^{-\beta}}{\eta}} - \lambda\left(\mathrm{e}^{-\frac{x^{-\beta}}{\eta}}\right)^2 &= u \\
\frac{4(1+\lambda)\lambda\,\mathrm{e}^{-\frac{x^{-\beta}}{\eta}} - 4\lambda^2\left(\mathrm{e}^{-\frac{x^{-\beta}}{\eta}}\right)^2}{4\lambda} &= u \\
(1+\lambda)^2 - (1+\lambda)^2 + 4(1+\lambda)\left(\lambda\,\mathrm{e}^{-\frac{x^{-\beta}}{\eta}}\right) - 4\lambda^2\left(\mathrm{e}^{-\frac{x^{-\beta}}{\eta}}\right)^2 &= 4\lambda u \\
(1+\lambda)^2 - 4(1+\lambda)\left(\lambda\,\mathrm{e}^{-\frac{x^{-\beta}}{\eta}}\right) + 4\lambda^2\left(\mathrm{e}^{-\frac{x^{-\beta}}{\eta}}\right)^2 &= (1+\lambda)^2 - 4\lambda u \\
\left((1+\lambda) - 2\lambda\,\mathrm{e}^{-\frac{x^{-\beta}}{\eta}}\right)^2 &= (1+\lambda)^2 - 4\lambda u \\
(1+\lambda) - 2\lambda\,\mathrm{e}^{-\frac{x^{-\beta}}{\eta}} &= \sqrt{(1+\lambda)^2 - 4\lambda u} \\
\frac{(1+\lambda) - \sqrt{(1+\lambda)^2 - 4\lambda u}}{2\lambda} &= \mathrm{e}^{-\frac{x^{-\beta}}{\eta}} \\
-\eta \log\left(\frac{(1+\lambda) - \sqrt{(1+\lambda)^2 - 4\lambda u}}{2\lambda}\right) &= x^{-\beta} \\
\left(-\eta \log\left(\frac{(1+\lambda) - \sqrt{(1+\lambda)^2 - 4\lambda u}}{2\lambda}\right)\right)^{-\frac{1}{\beta}} &= x.
\end{aligned}
$$

8.2. T^2 statistic

Algorithm to calculate T^2 statistic:	
Step 1	Estimate the β, η, λ parameters by ML, MM or LC methods,
Step 2	Take the estimatives from above step and find $\hat{\tilde{\kappa}}_2$ and $\hat{\tilde{\kappa}}_3$,
Step 3	Find sample LC: $\tilde{\kappa}_2$ and $\tilde{\kappa}_3$ through Log Moments,
Step 4	Calculate T^2 statistic with ML, MM or LC.

Below is the matrix $\mathbf{K_{3x3}}$:

$$\begin{aligned}
\mathbf{K_{3x3}} &= \mathbf{J_{3x3}^{\top}} \mathbf{M_{3x3}} \mathbf{J_{3x3}} \\
&= \begin{pmatrix} 1 & 0 & 0 \\ -2\mu_1 & 1 & 0 \\ -3(\mu_2 - 2\mu_1^2) & -3\mu_1 & 1 \end{pmatrix}^{\top} \begin{pmatrix} \tilde{\kappa}_2 & \tilde{\kappa}_3 + 2\tilde{\kappa}_1\tilde{\kappa}_2 & M_{1,3} \\ \tilde{\kappa}_3 + 2\tilde{\kappa}_1\tilde{\kappa}_2 & M_{2,2} & M_{2,3} \\ M_{3,1} & M_{3,2} & M_{3,3} \end{pmatrix} \begin{pmatrix} 1 & 0 & 0 \\ -2\mu_1 & 1 & 0 \\ -3(\mu_2 - 2\mu_1^2) & -3\mu_1 & 1 \end{pmatrix} \\
&= \begin{pmatrix} \tilde{\kappa}_2 & \tilde{\kappa}_3 & \tilde{\kappa}_4 \\ \tilde{\kappa}_3 & \tilde{\kappa}_4 + 2\tilde{\kappa}_2^2 & \tilde{\kappa}_5 + 6\tilde{\kappa}_2\tilde{\kappa}_3 \\ \tilde{\kappa}_4 & \tilde{\kappa}_5 + 6\tilde{\kappa}_2\tilde{\kappa}_3 & \tilde{\kappa}_6 + 9\tilde{\kappa}_2\tilde{\kappa}_4 + 9\tilde{\kappa}_3^2 + 6\tilde{\kappa}_2^3 \end{pmatrix},
\end{aligned}$$

where

$$\begin{aligned}
M_{1,3} &= \tilde{\kappa}_4 + 3\tilde{\kappa}_1\tilde{\kappa}_3 + 3\tilde{\kappa}_2^2 + 3\tilde{\kappa}_1^2\tilde{\kappa}_2 = M_{3,1}; \\
M_{2,2} &= \tilde{\kappa}_4 + 4\tilde{\kappa}_1\tilde{\kappa}_3 + 2\tilde{\kappa}_2^2 + 4\tilde{\kappa}_1^2\tilde{\kappa}_2; \\
M_{2,3} &= \tilde{\kappa}_5 + 5\tilde{\kappa}_1\tilde{\kappa}_4 + 9\tilde{\kappa}_2\tilde{\kappa}_3 + 9\tilde{\kappa}_1^2\tilde{\kappa}_3 + 12\tilde{\kappa}_1\tilde{\kappa}_2^2 + 6\tilde{\kappa}_1^3\tilde{\kappa}_2 = M_{3,2}; \\
M_{3,3} &= \tilde{\kappa}_6 + 6\tilde{\kappa}_1\tilde{\kappa}_5 + 15\tilde{\kappa}_2\tilde{\kappa}_4 + 15\tilde{\kappa}_1^2\tilde{\kappa}_4 + 9\tilde{\kappa}_3^2 + 54\tilde{\kappa}_1\tilde{\kappa}_2\tilde{\kappa}_3 + 18\tilde{\kappa}_1^3\tilde{\kappa}_3 + 15\tilde{\kappa}_2^3 + 36\tilde{\kappa}_1^2\tilde{\kappa}_2^2 + 9\tilde{\kappa}_1^4\tilde{\kappa}_2.
\end{aligned}$$

Based on (15), we obtain the asymptotic covariance matrix from LC ($\mathbf{K_{LC}}$) for TIW,

$$\mathbf{K_{LC}} = \begin{pmatrix} \tilde{\kappa}_4 + 2\tilde{\kappa}_2^2 & \tilde{\kappa}_5 + 6\tilde{\kappa}_2\tilde{\kappa}_3 \\ \tilde{\kappa}_5 + 6\tilde{\kappa}_2\tilde{\kappa}_3 & \tilde{\kappa}_6 + 9\tilde{\kappa}_2\tilde{\kappa}_4 + 9\tilde{\kappa}_3^2 + 6\tilde{\kappa}_2^3 \end{pmatrix} = \frac{1}{\beta^6} \begin{pmatrix} \tau_{2,2} & \tau_{2,3} \\ \tau_{3,2} & \tau_{3,3} \end{pmatrix},$$

where

$$\begin{aligned}
\tau_{2,2} &= \beta^2 \left\{ -\left(\lambda \log^4(2) \left(6\lambda^3 + 12\lambda^2 + 7\lambda + 1 \right) + \Psi^{(3)}(1) \right) + 2\left(-\left(\lambda \log^2(2)(\lambda + 1) + \Psi^{(1)}(1) \right) \right)^2 \right\}, \\
\tau_{2,3} &= \beta \left\{ -\left(\lambda \log^5(2) \left(24\lambda^4 + 60\lambda^3 + 50\lambda^2 + 15\lambda + 1 \right) + \Psi^{(4)}(1) \right) \right\} \\
&\quad + \beta \left\{ 6\left(-\left(\lambda \log^2(2)(\lambda + 1) + \Psi^{(1)}(1) \right) \right) \left(-\left(\lambda \log^3(2) \left(2\lambda^2 + 3\lambda + 1 \right) + \Psi^{(2)}(1) \right) \right) \right\} \\
&= \tau_{3,2}, \\
\tau_{3,3} &= -\left(\lambda \log^6(2) \left(120\lambda^5 + 360\lambda^4 + 390\lambda^3 + 180\lambda^2 + 31\lambda + 1 \right) + \Psi^{(5)}(1) \right) \\
&\quad + 9\left(-\left(\lambda \log^2(2)(\lambda + 1) + \Psi^{(1)}(1) \right) \right) \left(-\left(\lambda \log^4(2) \left(6\lambda^3 + 12\lambda^2 + 7\lambda + 1 \right) + \Psi^{(3)}(1) \right) \right) \\
&\quad + 9\left(-\left(\lambda \log^3(2) \left(2\lambda^2 + 3\lambda + 1 \right) + \Psi^{(2)}(1) \right) \right)^2 + 6\left(-\left(\lambda \log^2(2)(\lambda + 1) + \Psi^{(1)}(1) \right) \right)^3.
\end{aligned}$$

If $\mathbf{K_{LC}}$ is nonsingular, then

$$\mathbf{K_{LC}^{-1}} = \frac{\beta^6}{\tau_{33}\tau_{22} - \tau_{23}^2} \begin{pmatrix} \tau_{33} & -\tau_{32} \\ -\tau_{23} & \tau_{22} \end{pmatrix}.$$

Finally, T^2 statistic is given by

$$T^2 = n\left(\begin{bmatrix}\hat{\tilde{\kappa}}_2\\ \hat{\tilde{\kappa}}_3\end{bmatrix} - \begin{bmatrix}\tilde{\kappa}_2\\ \tilde{\kappa}_3\end{bmatrix}\right)^{\top} \widehat{\mathbf{K}}_{LC}^{-1} \left(\begin{bmatrix}\hat{\tilde{\kappa}}_2\\ \hat{\tilde{\kappa}}_3\end{bmatrix} - \begin{bmatrix}\tilde{\kappa}_2\\ \tilde{\kappa}_3\end{bmatrix}\right). \tag{15}$$

Further manipulation on the above equation leads to obtain

$$T^2 = \frac{n\beta^6}{\hat{\tau}_{3,3}\hat{\tau}_{2,2} - \hat{\tau}_{2,3}^2}\left[\hat{\tau}_{3,3}\left(\hat{\tilde{\kappa}}_2 - \tilde{\kappa}_2\right)^2 + \hat{\tau}_{2,2}\left(\hat{\tilde{\kappa}}_3 - \tilde{\kappa}_3\right)^2 - 2\hat{\tau}_{2,3}\left(\hat{\tilde{\kappa}}_2 - \tilde{\kappa}_2\right)\left(\hat{\tilde{\kappa}}_3 - \tilde{\kappa}_3\right)\right] \leq \chi^2_{2,\nu}.$$

Other way to obtain the asymptotic covariance matrix from ML ($\mathbf{K_{ML}}$) is by using the observed information matrix instead $\mathbf{M_{3x3}}$ as following

$$\mathbf{K_{ML}} = \mathbf{Z}^{\top}\mathbf{H}\mathbf{Z},$$

where $\mathbf{H} = -\frac{\partial^2 l(\beta,\eta,\lambda)}{\partial(\beta,\eta,\lambda)^{\top}\partial(\beta,\eta,\lambda)} = \begin{pmatrix}\mathbf{H}_{\beta\beta} & \mathbf{H}_{\beta\eta} & \mathbf{H}_{\beta\lambda}\\ \mathbf{H}_{\eta\beta} & \mathbf{H}_{\eta\eta} & \mathbf{H}_{\eta\lambda}\\ \mathbf{H}_{\lambda\beta} & \mathbf{H}_{\lambda\eta} & \mathbf{H}_{\lambda\lambda}\end{pmatrix}$, is the Hessian matrix from 3 and

$$\mathbf{Z} = \begin{pmatrix}\frac{\partial}{\partial\beta}\tilde{\kappa}_2 & \frac{\partial}{\partial\beta}\tilde{\kappa}_3\\ \frac{\partial}{\partial\eta}\tilde{\kappa}_2 & \frac{\partial}{\partial\eta}\tilde{\kappa}_3\\ \frac{\partial}{\partial\lambda}\tilde{\kappa}_2 & \frac{\partial}{\partial\lambda}\tilde{\kappa}_3\end{pmatrix} = \begin{pmatrix}\frac{2}{\beta^3}\left(\lambda\log^2(2)(\lambda+1) + \Psi^{(1)}(1)\right) & \frac{3\left(\lambda(2\lambda^2+3\lambda+1)\log^3(2)+\Psi^{(2)}(1)\right)}{\beta^4}\\ 0 & 0\\ -\frac{(2\lambda+1)\log^2(2)}{\beta^2} & -\frac{(6\lambda^2+6\lambda+1)\log^3(2)}{\beta^3}\end{pmatrix}.$$

Thus,

$$\mathbf{K_{ML}} = \frac{\mathbf{H}_{\beta\beta}\mathbf{H}_{\lambda\lambda} - \mathbf{H}_{\eta\lambda}^{\mathbf{2}}}{\beta^{\mathbf{8}}|\mathbf{L}|}\begin{pmatrix}4\beta^2\Psi^{(1)}(1)^2 & 6\beta^2\Psi^{(1)}(1)\Psi^{(2)}(1)\\ 6\beta\Psi^{(1)}(1)\Psi^{(2)}(1) & 9\Psi^{(2)}(1)^2\end{pmatrix},$$

$$|\mathbf{L}| = \mathbf{H}_{\beta\beta}(\mathbf{H}_{\eta\eta}\mathbf{H}_{\lambda\lambda} - \mathbf{H}_{\eta\lambda}^{\mathbf{2}}) + \mathbf{H}_{\beta\eta}(\mathbf{H}_{\beta\lambda}\mathbf{H}_{\eta\lambda} - \mathbf{H}_{\beta\eta}\mathbf{H}_{\lambda\lambda}) + \mathbf{H}_{\beta\lambda}(\mathbf{H}_{\beta\eta}\mathbf{H}_{\eta\lambda} - \mathbf{H}_{\beta\lambda}\mathbf{H}_{\eta\eta}).$$

Finally, the T^2 statistic by using $\mathbf{K_{ML}}$ is

$$T^2 = n\left(\begin{bmatrix}\hat{\tilde{\kappa}}_2\\ \hat{\tilde{\kappa}}_3\end{bmatrix} - \begin{bmatrix}\tilde{\kappa}_2\\ \tilde{\kappa}_3\end{bmatrix}\right)^{\top} \widehat{\mathbf{K}}_{ML}^{-1} \left(\begin{bmatrix}\hat{\tilde{\kappa}}_2\\ \hat{\tilde{\kappa}}_3\end{bmatrix} - \begin{bmatrix}\tilde{\kappa}_2\\ \tilde{\kappa}_3\end{bmatrix}\right). \tag{16}$$

We furnish the expression expanded

$$T^2 = \frac{n\hat{\beta}^6}{4}\left(\frac{1}{\hat{\beta}^2} - \frac{1}{\beta^2}\right)^2\left(\frac{|\hat{\mathbf{L}}|}{\mathbf{H}_{\hat{\beta}\hat{\beta}}\mathbf{H}_{\hat{\lambda}\hat{\lambda}} - \mathbf{H}_{\hat{\eta}\hat{\lambda}}}\right).$$

Acknowledgments

The research of Daniel Leonardo Ramírez Orozco was supported by the Brazilian Government through the Coordenação de Aperfeiçoamento de Pessoal de Nível Superior (CAPES) Cod. 001.

References

[1] M. V. Aarset. How to identify a bathtub hazard rate. *IEEE Transactions on Reliability*, 36(1):106–108, 1987.
[2] K. A. AL-Kadim and M. H. Mohammed. The cubic transmuted Weibull distribution. *Journal of University of Babylon*, 3:862–876, 2017.
[3] A. I. Al-Omari. The transmuted generalized inverse Weibull distribution in acceptance sampling plans based on life tests. *Transactions of the Institute of Measurement and Control*, 40(16):4432–4443, 2018.

[4] M. Ambrožič and L. Gorjan. Reliability of a Weibull analysis using the maximum-likelihood method. *Journal of materials science*, 46(6):1862–1869, 2011.
[5] T. W. Anderson. An introduction to multivariate statistical analysis. Technical report, Wiley New York, 1962.
[6] S. N. Anfinsen, A. P. Doulgeris, and T. Eltoft. Goodness-of-fit tests for multilook polarimetric radar data based on the Mellin transform. *IEEE Transactions on Geoscience and Remote Sensing*, 49(7):2764–2781, 2011.
[7] S. N. Anfinsen and T. Eltoft. Application of the matrix-variate Mellin transform to analysis of polarimetric radar images. *IEEE Transactions on geoscience and remote sensing*, 49(6):2281–2295, 2011.
[8] M. Bebbington, C.-D. Lai, and R. Zitikis. A flexible Weibull extension. *Reliability Engineering & System Safety*, 92(6):719–726, 2007.
[9] J. Bertrand, P. Bertrand, and J.-P. Ovarlez. The mellin transform, 1995. Handbook, 1995, 978-1420066524. ffhal-03152634.
[10] P. L. Butzer and S. Jansche. A direct approach to the Mellin transform. *Journal of Fourier Analysis and Applications*, 3(4):325–376, 1997.
[11] F. R. De Gusmao, E. M. Ortega, and G. M. Cordeiro. The generalized inverse weibull distribution. *Statistical Papers*, 52(3):591–619, 2011.
[12] Y. Delignon, R. Garello, and A. Hillion. Statistical modelling of ocean sar images. *IEE Proceedings-Radar, Sonar and Navigation*, 144(6):348–354, 1997.
[13] S. Dey, D. Kumar, M. Z. Anis, S. Nadarajah, and I. Okorie. A review of transmuted distributions. *Journal of the Indian Society for Probability and Statistics*, pages 1–65, 2021.
[14] B. Epstein. Some applications of the Mellin transform in statistics. *The Annals of Mathematical Statistics*, pages 370–379, 1948.
[15] A. J. Hallinan Jr. A review of the Weibull distribution. *Journal of Quality Technology*, 25(2):85–93, 1993.
[16] A. Henningsen and O. Toomet. maxlik: A package for maximum likelihood estimation in R. *Computational Statistics*, 26(3):443–458, 2011.
[17] H. Hotelling. The generalization of Student's ratio. In *Breakthroughs in statistics*, pages 54–65. Springer, 1992.
[18] P. Jain, C. Basu, and V. Panwar. On the (p, q)-Mellin transform and its applications. *Acta Mathematica Scientia*, 41(5):1719–1732, 2021.
[19] U. Jan, K. Fatima, and S. Ahmad. Transmuted exponentiated inverse Weibull distribution with application in medical sciences. *International Journal of Mathematics Trends and Technology (IJMTT)*, 50(3):160–167, 2017.
[20] D. Kececioglu. *Reliability engineering handbook*, volume 1. DEStech Publications, Inc, 2002.
[21] A. Keller, K. AZ, and K. ARR. Alternate reliability models for mechanical systems. 1982.
[22] M. S. Khan and R. King. Transmuted generalized inverse Weibull distribution. *Journal of Applied Statistical Science*, 20(3):213, 2012.
[23] M. S. Khan and R. King. A new class of transmuted inverse Weibull distribution for reliability analysis. *American Journal of Mathematical and Management Sciences*, 33(4):261–286, 2014.
[24] M. S. Khan and R. King. New generalized inverse Weibull distribution for lifetime modeling. *Communications for Statistical Applications and Methods*, 23(2):147–161, 2016.
[25] M. S. Khan, G. Pasha, and A. H. Pasha. Theoretical analysis of inverse Weibull distribution. *WSEAS Transactions on Mathematics*, 7(2):30–38, 2008.
[26] N. Kyurkchiev and S. Markov. On the hausdorff distance between the heaviside step function and verhulst logistic function. *Journal of Mathematical Chemistry*, 54(1):109–119, 2016.
[27] C. Lee, F. Famoye, and O. Olumolade. Beta-Weibull distribution: some properties and applications to censored data. *Journal of modern applied statistical methods*, 6(1):17, 2007.
[28] E. Lee and J. Wang. Tests of goodness of fit and distribution selection. *Statistical methods for survival data analysis*, 3:221–242, 2003.
[29] W. Q. Meeker, L. A. Escobar, and F. G. Pascual. *Statistical methods for reliability data*. John Wiley & Sons, 2021.
[30] F. Merovci, I. Elbatal, and A. Ahmed. Transmuted generalized inverse Weibull distribution. *arXiv preprint arXiv:1309.3268*, 2013.
[31] P. R. Nelson. Control charts for Weibull processes with standards given. *IEEE Transactions on Reliability*, 28(4):283–288, 1979.
[32] W. Nelson. Weibull analysis of reliability data with few or no failures. *Journal of Quality Technology*, 17(3):140–146, 1985.
[33] J.-M. Nicolas. Introduction aux statistiques de deuxième espèce: Applications des logs-moments et des logs-cumulants à l'analyse des lois d'images radar. *TS. Traitement du signal*, 19(3):139–167, 2002.
[34] J.-M. Nicolas. Application de la transformée de Mellin: étude des lois statistiques de l'imagerie cohérente. *Rapport de recherche, 2006D010*, 2006.
[35] K. Pearson. X. contributions to the mathematical theory of evolution.—ii. skew variation in homogeneous material. *Philosophical Transactions of the Royal Society of London.(A.)*, (186):343–414, 1895.
[36] R. R. Pescim, E. M. Ortega, G. M. Cordeiro, C. G. Demtrio, and G. Hamedani. The log-beta generalized half-normal regression model. *Journal of Statistical Theory and Applications*, 2013.
[37] M. M. Rahman, B. AL-Zahrani, S. H. Shahbaz, and M. Q. Shahbaz. Transmuted probability distributions: A review. *Pakistan Journal of Statistics and Operation Research*, pages 83–94, 2020.
[38] H. Rinne. *The Weibull distribution: a handbook*. Chapman and Hall/CRC, 2008.
[39] A. Saboor, H. S. Bakouch, and M. N. Khan. Beta sarhan–zaindin modified Weibull distribution. *Applied Mathematical Modelling*, 40(13-14):6604–6621, 2016.
[40] W. T. Shaw and I. R. Buckley. The alchemy of probability distributions: beyond Gram-Charlier expansions, and a skew-kurtotic-normal distribution from a rank transmutation map. *arXiv preprint arXiv:0901.0434*, 2009.
[41] V. P. Singh. On application of the weibull distribution in hydrology. *Water Resources Management*, 1(1):33–43, 1987.
[42] M. S. Suprawhardana and S. Prayoto. Total time on test plot analysis for mechanical components of the rsg-gas reactor. *Atom Indones*, 25(2):81–90, 1999.
[43] R. C. Team et al. R: A language and environment for statistical computing. 2013.
[44] R. Varadhan and P. Gilbert. Bb: An r package for solving a large system of nonlinear equations and for optimizing a high-

dimensional nonlinear objective function. *Journal of statistical software*, 32:1–26, 2010.
[45] J. M. Vasconcelos, R. J. Cintra, and A. D. Nascimento. Goodness-of-fit measures based on the Mellin transform for beta generalized lifetime data. *Mathematical Methods in the Applied Sciences*, 2021.
[46] W. Weibull et al. A statistical distribution function of wide applicability. *Journal of applied mechanics*, 18(3):293–297, 1951.
[47] T. Zaevski and N. Kyurkchiev. On some composite kies families: distributional properties and saturation in hausdorff sense. *Modern Stochastics: Theory and Applications*, pages 1–26, 2023.